Three-dimensional magnetic field of a superconducting quadrupole with rectangular coil blocks and constant-perimeter end windings

G. Dugan
Cornell University

In this note, I describe the use of the field calculation techniques outlined in CBN 96-5 to calculate the magnetic field of a quadrupole coil wound with a "constant perimeter" constraint in the ends. The coil is composed of three coil blocks, which have a rectangular two-dimensional cross section, as opposed to the cylindrical-sector shape associated with Rutherford cable. This note describes the details of the geometry needed to apply the CBN 96-5 model to this case, and gives some results for a constant-perimeter coil very similar to that currently proposed for the CESR Q1/Q2 quadrupole.

1. Rectangular Coil-block geometry

Figure 1 defines some quantities to be used to describe the rectangular coil cross section. The coil block is taken to be made from N flat cables, each of thickness d and width T. A given flat cable is located by specifying its azimuthal angle α, inner radius R, and inclination angle $\beta(\alpha)$ with respect to the x-axis. The cylindrical coordinates of an element of the cable at distance t along the width ($0<t<T$) are

$$\rho(\alpha,t)^2 = R^2 + t^2 + 2RtCos[\alpha - \beta(\alpha)]$$

$$Tan[\phi(\alpha,t)] = \frac{RSin[\alpha] + tSin[\beta(\alpha)]}{RCos[\alpha] + tCos[\beta(\alpha)]}$$

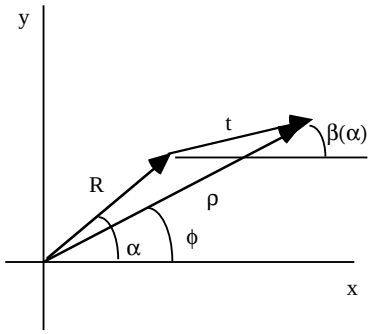

Fig. 1: Flat cable geometry

A complete cable block, made from N flat cables of width d each, has a width w=Nd. Fig. 2 shows a complete rectangular cable block, extending from α_0 to α_1, with fixed inner radius R_1. Generally the whole cable block has the same inclination angle β and inner radius R_1; for generality, however, I allow for β to vary with α. This allows the "rectangular" block to be wedge-shaped. If β varies with α, then of course the cable block width w must also vary with t. In what follows below, we shall concentrate on the rectangular block case, where w and β are fixed for a given coil block.

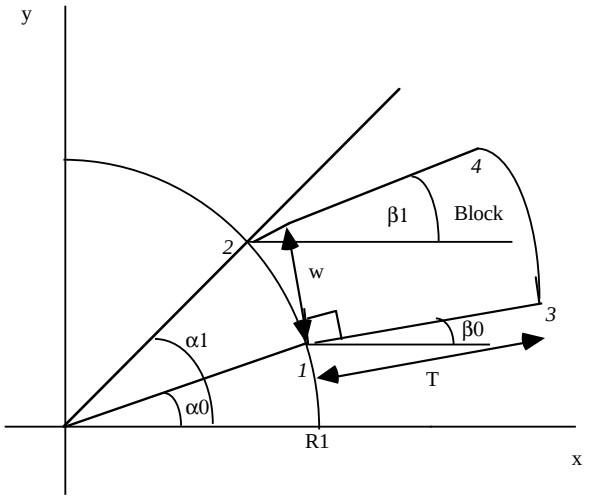

Fig 2. Cable block geometry

The start of the block is defined by R_1, α_0; The azimuthal angle of the end of the block is

$$\alpha_1 = \beta_1 + \mathrm{Sin}^{-1}\left(\mathrm{Sin}[\alpha_0 - \beta_1] + \frac{w\mathrm{Cos}[\beta_1 - \beta_0]}{R_1}\right).$$

The block extends at α_0 from point 1 to point 3, along the line shown; this is the distance T. At α_1, the block extends from point 2 to point 4, also a distance T. The points (1,2,3,4) in fig. 2 which define the cable block have cylindrical coordinates:

$$\{\rho_1,\phi_1\} = \{R_1,\alpha_0\};$$

$$\{\rho_2,\phi_2\} = \{R_1,\alpha_1\};$$

$$\{\rho_3,\phi_3\} = \{R_1^2 + T^2 + 2R_1T\mathrm{Cos}[\alpha_0 - \beta(\alpha)], \mathrm{Tan}^{-1}[\frac{R_1\mathrm{Sin}[\alpha_0] + T\mathrm{Sin}[\beta(\alpha_0)]}{R_1\mathrm{Cos}[\alpha_0] + T\mathrm{Cos}[\beta(\alpha_0)]}]\}$$

$$\{\rho_4,\phi_4\} = \{R_1^2 + T^2 + 2R_1T\mathrm{Cos}[\alpha_1 - \beta(\alpha_1)], \mathrm{Tan}^{-1}[\frac{R_1\mathrm{Sin}[\alpha_1] + T\mathrm{Sin}[\beta(\alpha_1)]}{R_1\mathrm{Cos}[\alpha_1] + T\mathrm{Cos}[\beta(\alpha_1)]}]\}$$

As the variable t ranges from 0 to T, and α ranges from α_0 to α_1, we span the whole coil block, and can calculate the cylindrical coordinates ρ,ϕ at each point from the above equations. Note that ρ_3 and ρ_4 are slightly different (typically by less than 1%)

2. Constant perimeter end constraints

Each flat cable must make a transition around the coil end in such a way as to keep the perimeter of the edges of the cable the same for all t from t=0 to t=T.

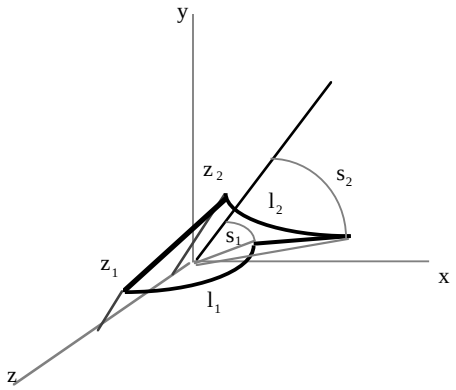

Fig. 3 Constant perimeter flat cable: $l_1 = l_2$.

Figure 3 shows a flat cable as it turns around the end of the magnet. The constant perimeter requirement is that the lengths l_1 and l_2 be equal.

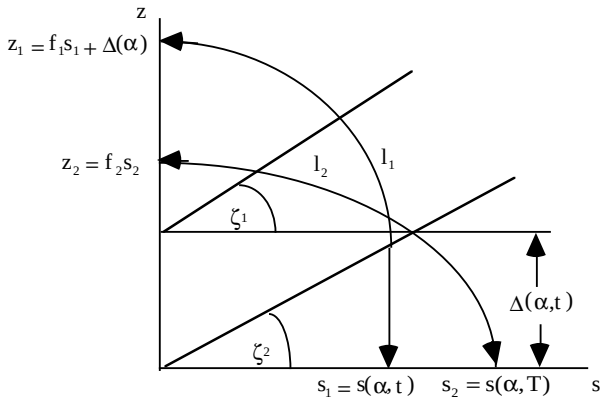

Fig 4. Coil layout at fixed α

In fig 4., the edges of the flat cable are shown in $s=\rho\theta$ vs. z space. ($\theta=\pi/4-\phi$). The flat coil is located at azimuth α, with inclination $\beta(\alpha)$. The edge with perimeter l_1 starts at t; the edge with perimeter l_2 starts at T. The arc-length distances s_1 and s_2 are

$$s_1 = s(\alpha,t) = \rho(\alpha,t)\left[\frac{\pi}{4} - \phi(\alpha,t)\right]$$
$$= \sqrt{R_1^2 + t^2 + 2R_1 t\,\mathrm{Cos}[\alpha-\beta(\alpha)]}\left[\frac{\pi}{4} - \mathrm{Tan}^{-1}\left(\frac{R_1\mathrm{Sin}[\alpha] + t\mathrm{Sin}[\beta(\alpha)]}{R_1\mathrm{Cos}[\alpha] + t\mathrm{Cos}[\beta(\alpha)]}\right)\right]$$

$$s_2 = s(\alpha,T) = \rho(\alpha,T)\left[\frac{\pi}{4} - \phi(\alpha,T)\right]$$
$$= \sqrt{R_1^2 + T^2 + 2R_1 T\,\mathrm{Cos}[\alpha-\beta(\alpha)]}\left[\frac{\pi}{4} - \mathrm{Tan}^{-1}\left(\frac{R_1\mathrm{Sin}[\alpha] + T\mathrm{Sin}[\beta(\alpha)]}{R_1\mathrm{Cos}[\alpha] + T\mathrm{Cos}[\beta(\alpha)]}\right)\right]$$

On the surface of a cylinder, each end of the flat coil follows an ellipse as shown in fig. 4. The end at t=T starts at s_2 and intersects the z-axis at $z_2=f_2 s_2$. The end at t starts at s_1, follows a straight line (on the cylindrical surface) a distance $\Delta(\alpha,t)$, and then follows an ellipse, intersecting the z-axis at $z_1=f_1 s_1+\Delta(\alpha,t)$. The distance $\Delta(\alpha,t)$ and the eccentricities of the ellipses f_1,f_2 are adjusted so as to make the perimeters (path lengths in fig.4) l_1 and l_2 equal. In general, the curves can be parameterized using the angle ζ shown in the figure as

$$s_1(\zeta_1) = s_1\mathrm{Cos}[\zeta_1]$$
$$z_1(\zeta_1) = f_1 s_1\mathrm{Sin}[\zeta_1] + \Delta(\alpha,t)$$
$$s_2(\zeta_2) = s_2\mathrm{Cos}[\zeta_2]$$
$$z_2(\zeta_2) = f_2 s_2\mathrm{Sin}[\zeta_2]$$

The differential path length is $dl^2 = ds^2 + dz^2$ and

$$ds = -s\mathrm{Sin}[\zeta]d\zeta$$
$$dz = fs\mathrm{Cos}[\zeta]d\zeta$$

which makes the differential along the elliptical path

$$dl = s\sqrt{\mathrm{Sin}^2[\zeta] + f^2\mathrm{Cos}^2[\zeta]}$$

The total path lengths shown in fig.4 are then

$$l_1 = \int dl_1 = \Delta(\alpha,t) + s_1\int_0^{\frac{\pi}{2}}\sqrt{\mathrm{Sin}^2[\zeta] + f_1^2\mathrm{Cos}^2[\zeta]}d\zeta$$

$$l_2 = \int dl_2 = s_2\int_0^{\frac{\pi}{2}}\sqrt{\mathrm{Sin}^2[\zeta] + f_2^2\mathrm{Cos}^2[\zeta]}d\zeta$$

In terms of the complete elliptic integral

$$E(m) = \int_0^{\frac{\pi}{2}}\sqrt{1 - m\mathrm{Sin}^2[\phi]}d\phi$$

$$g(m) = mE(m)$$

we obtain

$$l_1 = \Delta(\alpha,t) + s_1 g(f_1)$$
$$l_2 = s_2 g(f_2)$$

For a constant perimeter, we must have $l_1 = l_2$:

$$\Delta(\alpha,t) + s_1 g(f_1) = s_2 g(f_2)$$

which specifies a relation between f_1, f_2, and $\Delta(\alpha,t)$. We consider only cases in which $f_1=f_2=f$ is independent of t; then

$$\Delta(\alpha,t) = (s_2 - s_1)g(f) = (s(\alpha,T) - s(\alpha,t))g(f)$$

With this form for $\Delta(\alpha,t)$, we will have a constant perimeter for the flat coil. In general, the ellipticity parameter f will be a function of α. The form of $f(\alpha)$ is fixed if we assume a "constant width" coil.

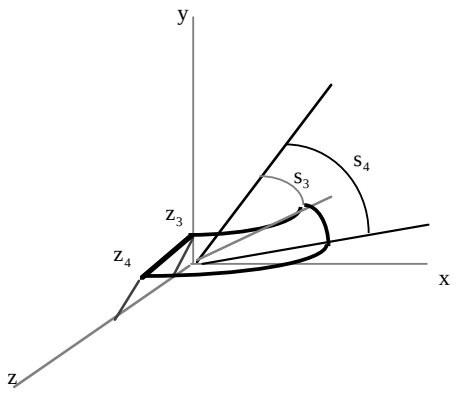

Fig 5. Coil block edge at t=T

Fig. 5 shows the layout of a piece of the t=T edge of the coil block as it goes around the magnet end; the piece varies in α from α_1 to α.

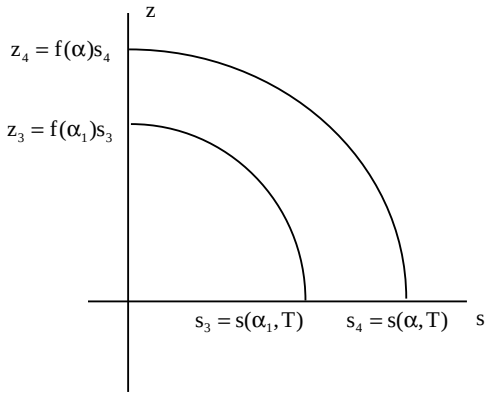

Fig. 6: Coil end layout at fixed t=T

Fig 6. shows the same layout, in the s-z surface. We have

$$s_3 = s(\alpha_1, T)$$
$$s_4 = s(\alpha, T)$$

The z-distances are

$$z_3 = f(\alpha_1)s_3$$
$$z_4 = f(\alpha)s_4$$

The coil block width is s_4-s_3. If this width is held constant as the coil block edge goes around the end of the magnet, then we must have

$$z_4 - z_3 = f(\alpha)s_4 - f(\alpha_1)s_3 = s_4 - s_3$$
$$f(\alpha) = 1 + \frac{s_3(f(\alpha_1) - 1)}{s_4} = 1 + \frac{s(\alpha_1, T)(f - 1)}{s(\alpha, T)}$$

in which we have set $f(\alpha_1) = f$. The quantity f is the ratio of the half-axis of the "upper ellipse" at α_1 to the arc length s_3:

$$f = \frac{\text{Half} - \text{axis of upper ellipse of cable block}}{\text{Arc length from } 45^o \text{ to cable block}} = \frac{z_3}{s_3}$$

The constant-perimeter requirement then becomes

$$\Delta(\alpha, t) = (s(\alpha, T) - s(\alpha, t))g(1 + \frac{s(\alpha_1, T)(f - 1)}{s(\alpha, T)})$$

A cross-sectional cut of the coil block in a plane formed by the z-axis and a line at 45^o in the x-y plane is shown in figure 7:

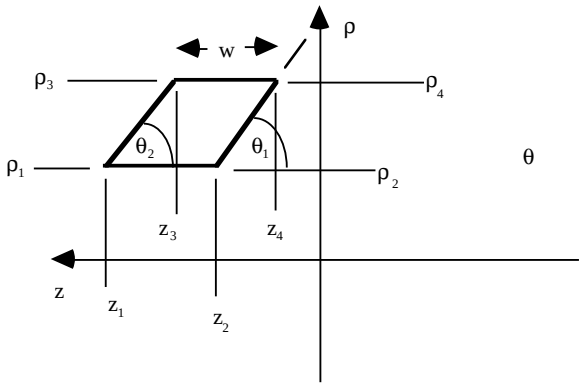

Fig. 7: Inclination angles θ_1,θ_2

In general, the z-coordinate of an element of the block at (α,t) is given by

$$z(\alpha,t) = \Delta(\alpha,t) + f(\alpha)s(\alpha,t)$$

In fig. 7, the edges of the coil block are given by

$$z_1 = z(\alpha_0,0) = \Delta(\alpha_0,0) + f(\alpha_0)s(\alpha_0,0)$$
$$z_2 = z(\alpha_1,0) = \Delta(\alpha_1,0) + f(\alpha_1)s(\alpha_1,0)$$
$$z_3 = z(\alpha_0,T) = \Delta(\alpha_0,T) + f(\alpha_0)s(\alpha_0,T) = f(\alpha_0)s(\alpha_0,T)$$
$$z_4 = z(\alpha_1,T) = \Delta(\alpha_1,T) + f(\alpha_1)s(\alpha_1,T) = f(\alpha_1)s(\alpha_1,T)$$

The inclination angle of the coil block in this plane is given by

$$\mathrm{Tan}[\theta_1] = \frac{\rho_4 - \rho_2}{z_4 - z_2} = \frac{\rho_4 - \rho_2}{f(\alpha_1)s(\alpha_1,T) - \Delta(\alpha_1,0) - f(\alpha_1)s(\alpha_1,0)} = \frac{\rho_4 - \rho_2}{f\big(s(\alpha_1,T) - s(\alpha_1,0)\big) - \Delta(\alpha_1,0)}$$

Since

$$\Delta(\alpha_1,0) = (s(\alpha_1,T) - s(\alpha_1,0))g(f)$$

we have

$$\mathrm{Tan}[\theta_1] = \frac{\rho_4 - \rho_2}{\big(f - g(f)\big)\big(s(\alpha_1,T) - s(\alpha_1,0)\big)}$$

and

$$\mathrm{Tan}[\theta_2] = \frac{\rho_3 - \rho_1}{z_3 - z_1} = \frac{\rho_3 - \rho_1}{f(\alpha_0)s(\alpha_0,T) - \Delta(\alpha_0,0) - f(\alpha_0)s(\alpha_0,0)} = \frac{\rho_3 - \rho_1}{f(\alpha_0)\big(s(\alpha_0,T) - s(\alpha_0,0)\big) - \Delta(\alpha_0,0)}$$

3. Implementation in the model described in CBN 96-5

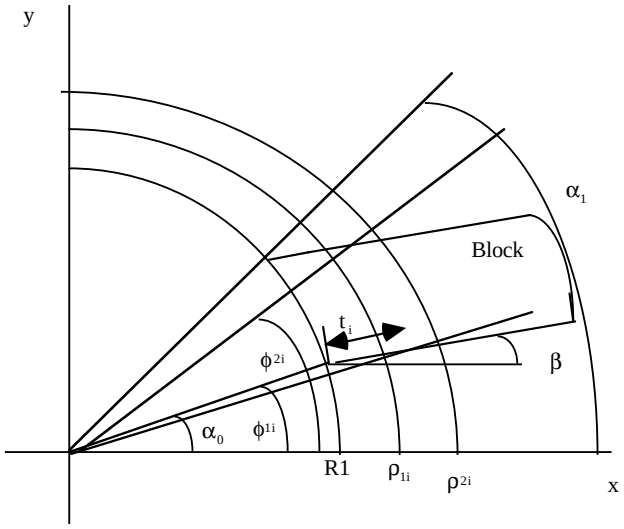

Fig 8: Division of coil block into segments

The model described in CBN 96-5 can calculate the field from coil blocks which are "wedge-shaped" in azimuthal cross-section, and extend in azimuth from ϕ_1 to ϕ_2 ,and in radius from R_1 to R_2. Each such coil block has a straight section of length L, with ends composed of straight extensions of length ΔL, and a "constant-width" coil end geometry with ellipse parameter f (for the inner edge of the ellipse). In order to model the rectangular, constant perimeter coil block described above, we divide the rectangular block into M segments in t, of width $\delta t=T/M$, where $t_i = (i-0.5)*T/M$ is the center of the segment, and i runs from 1 to M. The radial extent of each segment is from ρ_{1i} to ρ_{2i}, where

$$\rho_{1i} = \sqrt{R_1^2 + (t_i - \frac{\delta t}{2})^2 + 2R_1(t_i - \frac{\delta t}{2})\mathrm{Cos}[\alpha_0 - \beta[\alpha_0]]}$$

$$\rho_{2i} = \sqrt{R_1^2 + (t_i + \frac{\delta t}{2})^2 + 2R_1(t_i + \frac{\delta t}{2})\mathrm{Cos}[\alpha_0 - \beta[\alpha_0]]}$$

The azimuthal extent of each segment is taken as running from ϕ_{1i} to ϕ_{21}, where

$$\phi_{1i} = \mathrm{Tan}^{-1}\left[\frac{R_1\mathrm{Sin}[\alpha_0] + t_i\mathrm{Sin}[\beta[\alpha_0]]}{R_1\mathrm{Cos}[\alpha_0] + t_i\mathrm{Cos}[\beta[\alpha_0]]}\right]$$

$$\phi_{2i} = \mathrm{Tan}^{-1}\left[\frac{R_1\mathrm{Sin}[\alpha_1] + t_i\mathrm{Sin}[\beta[\alpha_1]]}{R_1\mathrm{Cos}[\alpha_1] + t_i\mathrm{Cos}[\beta[\alpha_1]]}\right]$$

We will use the model of CBN 96-5 for each of these segments, and then superimpose the results. To describe the constant-perimeter ends, we use the ellipse parameter f; the constant-perimeter requirement is imposed by giving each segment a length extension

$$\Delta L_i = \frac{\Delta(\alpha_1, t_i) + \Delta(\alpha_0, t_i)}{2} + z_0$$

in which z_0 is the overall shift of the whole coil block, if any. Because $\Delta(\alpha,t)$ is only weakly dependent on α, the average indicated above introduces little error.

Magnetic field and harmonics:

Let n be the index of the coil block (n runs from 1 to N), and let i be the index of the segment of the nth block (i runs from 1 to M(n)). The azimuthal extent of this segment is from $\phi_{1i}(n)$ to $\phi_{2i}(n)$; the radial extent is from $\rho_{1i}(n)$ to $\rho_{2i}(n)$. The magnetic field due to this segment is

$$\Delta\vec{B}_i(n) = \frac{\mu_0}{4\pi}\frac{(\Delta NI)_i(n)}{\rho_{2i}(n) - \rho_{1i}(n)}\frac{\vec{\vec{I}}[\rho, \phi, z + \Delta L_i(n)]_{\phi_{1i}(n), \phi_{2i}(n), f(n), L(n)}}{\phi_{s,i}(n)}$$

The field in harmonic form is given by

$$\Delta\vec{B}_i(r;k)(n) = \frac{4\mu_0}{\pi}\frac{(\Delta NI)_i(n)}{\rho_{0i}^2(n)\phi_{s,i}(n)}\rho_0\vec{\vec{V}}_k(\phi)\left[\frac{\rho}{\rho_0}\right]^{2k-1+2r}\sigma_i(n)\bullet\vec{\vec{\delta}}(r,k,\chi+\frac{\Delta L_i(n)}{\rho_{0i}(n)})_{\phi_{1i}(n),\phi_{2i}(n),f(n),s(n)}$$

in which

$$(\Delta NI)_i(n) = \frac{NI(n)}{M(n)}$$

is the ratio of the number of amp-turns in block n to the number of segments, M(n), and

$$\sigma_i(n) = Sin[\phi_{s,i}(n)]Cos[2\phi_{1i}(n)+\phi_{s,i}(n)]$$

We are assuming that the current is constant in each coil block. The total field for N coil blocks is then

$$\vec{B}_{tot} = \frac{\mu_0}{4\pi}\sum_{n=1}^{N}\frac{NI(n)}{M(n)}\sum_{i=1}^{M(n)}\frac{\vec{\tilde{I}}[\rho,\phi,z+\Delta L_i(n)]_{\phi_{1i}(n),\phi_{2i}(n),f(n),L(n)}}{(\rho_{2i}(n)-\rho_{1i}(n))\phi_{s,i}(n)}$$

and in harmonic expansion form,

$$\vec{B}_{tot} = \frac{4\mu_0}{\pi}\rho_0\sum_{n=1}^{N}\frac{NI(n)}{M(n)}\sum_{i=1}^{M(n)}\frac{\sigma_i(n)}{\rho_{0i}^2(n)\phi_{s,i}(n)}\sum_{k,r}\vec{\vec{V}}_k(\phi)\left[\frac{\rho}{\rho_0}\right]^{2k-1+r}\bullet\vec{\vec{\delta}}(r,k,\chi+\frac{\Delta L_i(n)}{\rho_{0i}(n)})_{\phi_{1i}(n),\phi_{2i}(n),f(n),s(n)}$$

In terms of the gradient G, we have

$$\vec{B}_{tot} = G\rho_0\sum_{n=1}^{N}\frac{1}{Q}\frac{NI(n)}{M(n)}\sum_{i=1}^{M(n)}\frac{\sigma_i(n)}{\rho_{0i}^2(n)\phi_{s,i}(n)}\sum_{k,r}\vec{\vec{V}}_k(\phi)\left[\frac{\rho}{\rho_0}\right]^{2k-1+r}\bullet\vec{\vec{\delta}}(r,k,\chi+\frac{\Delta L_i(n)}{\rho_{0i}(n)})_{\phi_{1i}(n),\phi_{2i}(n),f(n),s(n)}$$

where the gradient is given by

$$G = \frac{4\mu_0}{\pi}Q = \frac{4\mu_0}{\pi}\sum_{n=1}^{N}\frac{NI(n)}{M(n)}\sum_{i=1}^{M(n)}\frac{\sigma_i(n)}{\rho_{0i}^2(n)\phi_{s,i}(n)}$$

The integrated field in harmonic form is

$$\int\vec{B}_{tot}dz = G\rho_0\sum_{n=1}^{N}\frac{1}{Q}\frac{NI(n)}{M(n)}\sum_{i=1}^{M(n)}\frac{\sigma_i(n)}{\rho_{0i}(n)\phi_{s,i}(n)}\sum_{k,r}\vec{\vec{V}}_k(\phi)\left[\frac{\rho}{\rho_0}\right]^{2k-1+r}\bullet\vec{\vec{\delta}}(r,k)_{\phi_{1i}(n),\phi_{2i}(n),f(n),s(n)}$$

The integrated harmonics are

$$L_{eff}b_{2k} = \sum_{n=1}^{N}\frac{1}{Q}\frac{NI(n)}{M(n)}\sum_{i=1}^{M(n)}\frac{\sigma_i(n)}{\rho_{0i}(n)\phi_{s,i}(n)}\left[2\bar{\delta}_\rho^{tot,end}(0,k)+\bar{\delta}_\rho^{tot,body}(0,k)\right]_{\phi_{1i}(n),\phi_{2i}(n),f(n),s(n)}$$

$$b_{2k} = \frac{1}{QL_{eff}}\sum_{n=1}^{N}\frac{NI(n)}{M(n)}\sum_{i=1}^{M(n)}\frac{\sigma_i(n)}{\rho_{0i}(n)\phi_{s,i}(n)}\left[\frac{\rho_0}{\rho_{0i}(n)}\right]^{2k-2}\left[s_i(n)\frac{Sin[2k\phi_{2i}(n)]-Sin[2k\phi_{1i}(n)]}{2k}+2(-1)^{\frac{k-1}{2}}\bar{I}_i(n;k)\right]$$

in which

$$\bar{I}_i(n;k) = \int_0^{\phi_{s,i}(n)}d\delta(f(n)\theta_{1i}(n)+\delta)\int_0^{\frac{\pi}{2}}d\alpha Sin[2kh_i(n;\alpha,\delta)]Sin[\alpha]$$

The effective length is

$$L_{eff} = \frac{1}{Q}\sum_{n=1}^{N}\frac{NI(n)}{M(n)}\sum_{i=1}^{M(n)}\frac{\sigma_i(n)}{\rho_{0i}(n)\phi_{s,i}(n)}\left[s_i(n)\frac{Sin[2\phi_{2i}(n)]-Sin[2\phi_{1i}(n)]}{2}+2\bar{I}_i(n;1)\right]$$

4. Results for a Q1/Q2 candidate design

A three-block coil design is being considered for the CESR Q1/Q2 superconducting IR quadrupole being produced by TESLA Engineering for Cornell. The basic geometrical parameters of the design are given in table 1. The common body length is 440 mm; the coil develops a field gradient of 47.96 T/m, with 445.9 kAmp turns. The nominal TESLA design contains 364 turns, and so requires 1225 A to get this field gradient. The effective length is 649.4 mm.

Table 2 gives the integrated harmonic content. The harmonics are all well within the specified tolerances.

Coil block #	**1**	**2**	**3**
R_1 (mm)	92.05	92.05	92.05
T(mm)	38.68	38.68	38.68
w(mm)	22.1	14.7	11
NI(kAmp)	205.8	137.2	102.9
α_0(rad)	0.0005	.262	.461
β(rad)	0.0	.2281	.5170
α_1(rad)	.242	.422	.581
ρ_1 (mm)	92.05	92.05	92.05
ρ_2 (mm)	92.05	92.05	92.05
ρ_3 (mm)	130.73	130.715	130.687
ρ_4 (mm)	129.934	130.216	130.675
ϕ_1(rad)	0.0	.262	.461
ϕ_2(rad)	.242	.422	.581
ϕ_3(rad)	0.0	.252	.478
ϕ_4(rad)	.171	.365	.562
f	1.186	1.184	1.263
z_0 (mm)	29.24	9.87	4.33
Overall length(mm)	767	643	555.6

Table 1: Geometrical parameters

Harmonic number (k)	**1**	**3**	**5**	**7**
b_{2k}	10000	2.0	-.223	0.137
$\hat{b}_{2k}$	387	.0003	-.001	.001

Table 2: Harmonic content of the field (in units; 1 unit=10^{-4})

Finally, we list in table 3 the peak fields in the body and ends for each coil block. Comparing these numbers with the 2-coil design described in CBN 96-5, we see that the peak fields in the ends have been reduced by 0.3 T, and the peak body fields are down by close to 0.5 T. This is due in part to the use of three coils, rather than two as in the CBN 96-5 design, and also to the fact that a smaller inner coil radius has been used.

Coil block #	**1**	**2**	**3**
End peak field (T)	3.11	4.19	5.41
ρ (mm)	108.1	108.3	108.2
ϕ (rad)	.767	.771	.768
z(mm)	-132	-80.4	-43.6
Body peak field (T)	4.45	3.85	5.04
ρ (mm)	92.1	104.1	104.8
ϕ (rad)	.373	.397	.574
z(mm)	267	245	232

Table 3: Peak fields in the coils

For a more complete comparison of this design with other magnets, we present in tables 4 through 9 various magnet parameters for this design and those of similar magnets, calculated as outlined in CBN 95-12. The peak field for this design (called "CESR Q1/Q2") includes the end field enhancement, the effect of skew quadrupole winding (as in CBN 95-13), and the effect of the CLEO solenoid field (in the body only). Even including all these effects, the design has margin in excess of 40%, because of the generous use of high-quality superconductor.

Descriptor	ISR quads	LEP quads	FNAL quads	RHIC quads	LEP200 quads	CESR Q1/Q2
Turns/pole	290	184	275	27	200	**364**
Wire area (mm^2)	6.4	6.4	4.2	11.9	5.8	**6.3**
a1 (mm)	115	90	75	65	80	**92**
a2(mm)	*143*	*112*	*100*	*74*	*104*	***131***
Re(mm)	200	-----	153	90	-----	------
I (amp)	1600	1600	905	5000	1900	**1225**
g(T/m)	*43*	*38.2*	*48*	*50*	*60*	***48***
J(amp/mm2)	*250*	*250*	*215*	*420*	*327*	***195***
B-peak(T)	*5.9*	*4.2*	*4.1*	*3.95*	*5.7*	***5.8***
B-iron (T)	*2.56*	----	*1.45*	*2.4*	-----	----
length(m)	.7	2	2.8	1.44	2	**.6**
L(H)	*.27*	*.26*	*.88*	*.006*	*.3*	***.30***
W-stored (kJ)	*345*	*330*	*360*	*73*	*535*	***227***

Table 4
Model design parameters

Quadrupole	T_0 ^oK	B_0 T	J_{c0} A/mm^2	T_b ^oK	B_{op}= Bpeak T	$T_c(B_{op})$ ^oK	$B_c(T_b)$ T	$J_c(B_{op},T_b)$ A/mm^2
ISR quads	4.2	5	1300	4.3	5.9	6.7	10.5	1038
LEP quads	4.2	5	1300	4.3	4.2	7.5	10.5	1452
CESR Q1/Q2	**4.5**	**5**	**2660**	**4.6**	**5.8**	**6.8**	**10.04**	**2146**
FNAL quads	4.2	5	1300	4.6	4.2	7.5	10	1328
RHIC quads	4.2	5.6	2300	4.6	3.9	7.6	10	2783
LEP 200 Quads	4.3	5	1400	4.3	5.7	6.8	10.5	1230

Table 5
Critical Temperatures, Fields and Current Densities

Quadrupole	T_{bath} ^oK	B_{peak} T	I_{op} A	$I_c(B_{op},T_b)$ A/mm^2	I_{quench} A	margin %	ΔT ^oK
ISR quads	4.3	5.9	1600	2460	1887	18	0.8
LEP quads	4.3	4.1	1600	3442	2365	47.8	1.7
CESR Q1/Q2	**4.6**	**5.8**	**1225**	**2709**	**1722**	**40.5**	**1.5**
FNAL quads	4.6	4.1	905	1992	1327	46	1.6
RHIC quads	4.6	3.9	5000	11831	7690	53.8	1.7
LEP 200 quads	4.3	5.7	1900	2641	2182	15	0.7

Table 6
Current and temperature margins

Quadrupole	J_{op} (A/mm^2)	P (mm)	G_c(mwatt/mm^3)	α	l_{min} (mm)
ISR quads	675	10.8	30	7.2	29
LEP quads	675	10.8	30	5.4	33
CESR Q1/Q2	**682**	**9.97**	**16**	**4.55**	**38**
FNAL quads	603	7	22	4.5	37
RHIC quads	1176	73.5	82	4.4	19
LEP 200 quads	884	8.9	51	13	23

Table 7
Cryostability parameters

Quadrupole	v_z (m/sec)	t'_Q(sec)	$T_{max}(^oK)$	$V_{max}(V)$
ISR quads	8.5	.75	492	700
LEP quads	7.4	.62	339	803
CESR Q1/Q2	**7.0**	**.961**	**303**	**477**
FNAL quads	6.8	.72	255	1328
RHIC quads	13	.23	381	152
LEP 200 quads	11	.42	450	1650

Table 8
Quench parameters

Quadrupole	Azimuthal force/length (N/mm) $r=a_1$, $\phi=\phi_1$.	Radial force/length (N/mm) $r=a_1$, $\phi=0$	Azimuthal pressure(N/mm^2) $r=a_1$, $\phi=\phi_1$.	Radial pressure (N/mm^2) $r=a_1$, $\phi=0$
ISR quads	8.5	7.2	3.5	3.0
LEP quads	6.0	4.8	2.5	2.0
CESR Q1/Q2	**5.2**	**4.9**	**2.1**	**1.96**
FNAL quads	3.3	2.9	1.4	1.2
LEP 200 quads	9.7	7.9	3.7	3.0

Table 9
Electromagnetic Forces

5. Direct comparison with ROXEI program

Finally, for the Q1/Q2 design described above, we present in table 10 a direct comparison between the fields calculated by the techniques described here and in CBN 96-5, and the fields calculated by the program ROXEI, which is being used by TESLA to design the quadrupoles. The field points chosen are all inside the coil. ROXEI does a direct Biot-Savart integration over the exact geometry of the wire array, but omits the field contribution from the strand which passes through the field point, so we might expect some small difference due to this. Other differences may be due to approximations used in the model geometry. In general, the results are seen to agree to typically better than 0.1 T.

			ROXEI			This Paper			Diff:(This Paper-ROXEI)		
x	y	z	B_x	B_y	B_z	B_x	B_y	B_z	ΔB_x	ΔB_y	ΔB_z
92.9	8.4	53.84	-.51	-4.21	0.	-.50	-4.19	0.	.01	.02	0
92.8	8.6	-68.1	-.50	-3.49	.23	-.64	-3.57	.20	–.14	–.08	–.03
69.5	63.5	-154	.11	-.07	1.85	.12	-.05	1.74	.01	.02	–.11
85.9	37.3	-15.	-2.31	-3.89	.17	-2.27	-3.88	.16	.04	.01	–.01
81.9	45.1	-72.5	-2.29	-3.20	1.32	-2.3	-3.10	1.27	–.01	.1	–.05
84.6	50.	-28.6	-3.89	-3.62	.37	-3.97	-3.68	.40	–.08	–.06	.03
78.1	64.7	-43.5	-3.75	-3.66	.73	-3.67	-3.58	.73	.08	–.08	0

Table10:
Comparison of ROXEI fields and fields calculated by the technique described in this paper